J. Cosmet. Sci., 75.2, 128–145 (March/April 2024)

Improved Photostability and Skin Retention of Avobenzone Encapsulated in Compatible Nanostructured Lipid Carriers

ISABELLY PAULA SOUSA, AMANDA CECÍLIA TEODORO LANDIM, BÁRBARA CRISTINA CAMPOS RIBEIRO, EMILIO RAMOS CINTRA, LORENA MAIONE SILVA, THAIS LEITE NASCIMENTO, ELIANA MARTINS LIMA, LUÍS ANTÔNIO DANTAS SILVA AND DANIELLE GUIMARÃES ALMEIDA DINIZ
Laboratory of Pharmaceutical Technology and Drug Delivery Systems, Federal University of Goias, Brazil (I.P.S., A.C.T.L., B.C.C.R., E.R.C., L.M.S., T.L.N., E.M.L., L.A.D.S., D.G.A.D.)
State University of Goias, Brazil (L.M.S.)

Accepted for publication February 28, 2024.

Synopsis

Avobenzone (AVB) is an organic filter acting in the UVA spectrum. To exert its photoprotective effect, AVB must be protected from UV radiation since it can suffer photoisomerization and incur adverse effects, such as endocrine and metabolic disruption. Nanostructured carriers are an interesting strategy for protecting the molecule and reducing skin permeation. This study aimed to improve AVB photostability and skin retention through encapsulation in nanostructured lipid carriers. Our results showed that nanoencapsulation in carnauba wax-nanostructured lipid carriers prepared with compatible lipid excipients proved to be an efficient strategy in preventing AVB photo-instability. The formulation showed improved skin retention, could be further investigated as a carrier to overcome AVB limitations as a long-wave UVA filter, and may contribute to improving the efficiency and safety of this active cosmetic ingredient.

INTRODUCTION

Nonmelanoma skin cancer is the most common human malignancy worldwide, with increasing yearly incidence rates.[1] Even with this high incidence, the disease has low mortality and a high probability of remission. Some important risk factors are related to the disease, such as genetic predisposition, skin phenotypes, and prolonged exposure to UV radiation without proper use of UV protection.[2,3] There is a growing need for more effective topical sunscreens to prevent the harmful effects of UV radiation on human skin.[4] While most sunscreens provide excellent protection against UVB radiation, adequate protection against UVA radiation is becoming increasingly necessary.[5] Studies highlight the significant role played by UVA radiation in sunlight-induced skin damage and changes, such as immunosuppression, DNA mutations, lipid and protein oxidative damage, increased epidermal ferritin expression, skin photoaging, and decreased skin

*Address all correspondence to Danielle Guimarães Almeida Diniz, danielle_diniz@ufg.br

hydration and elasticity.[6–8.] Through the generation of singlet oxygen, UVA radiation can induce the expression of matrix metalloproteinases that destroy connective tissue.[9] In this context, the availability of sunscreens with broader protection is an increasing consumer concern. Although most available commercial formulations have a variety of UVB filters, the number of UVB filters that are also effective UVA absorbers are rare, and they often present poor performance or are not photostable.

In 2019, the American Regulatory Agency Food and Drug Administration published regulations for products containing sunscreens, providing for their classification regarding the safety of filters that are marketed in the USA, classifying them as totally safe, unsafe, and requiring additional research.[10] Among those that require further research is butyl methoxydibenzoylmethane, also known as avobenzone (AVB).[10] AVB is a chemical UV filter associated with UVA protection. It is presented as a mixture of two tautomeric forms: enol and keto.[11] Chemical equilibrium between the two isoforms favors the enol form in almost all media due to its ability to form hydrogen bonds. The enol form absorbs in the UVA spectrum and is responsible for the UVA protection effect. Under irradiation, the enol form in solution photoisomerizes to the keto form, causing a large decrease in absorption. The keto form mainly absorbs in the UVC spectrum region, losing its UVA protective effect.[11,12]

Photostabilization is critical to the development of sunscreen formulations. Studies have shown that the use of nanotechnology in photoprotective formulations can improve the photo stability of some filters.[13,14] Formulations of lipid nanoparticles containing AVB have been evaluated for their ability to absorb UV radiation and their UVA protection factor after irradiation.[14] Type, physical properties, and chemical nature of lipid-based excipients may influence the physicochemical properties and stability of the lipid carriers,[15,16] as well as their interaction with biological systems.[17,18] Therefore, the screening of the excipients has been described to ensure the development of safe, stable, and efficient lipid-based formulations.[19,20] In this study, we used thermogravimetry (TG/DTG), differential thermal analysis (DTA), and Fourier-transform infrared spectroscopy (FTIR) techniques to evaluate the interaction between AVB and lipid excipients and to select the most suitable components for a rational nanostructured lipid carrier (NLC) design.

In the development of photoprotective formulations minimal skin permeation is required, since the exposure to many organic sunscreens has been associated with several adverse effects, such as endocrine[21] and metabolic disruption.[22,23] Besides the safety concern, the search for sunscreens that are stable, and thus maintain the photoprotective ability of the formulation, mobilizes the investigation of new applications, methods, and technologies applied to photoprotective formulations. In this work, we designed a NLC formulation encapsulating AVB, and evaluated its photostability against UV radiation and its ability to reduce the cutaneous penetration of AVB, favoring its retention on the skin surface.

MATERIALS

Avobenzone was purchased from Symrise AG (Holzminden, Germany). Avobenzone standard was purchased from Sigma-Aldrich (Missouri, USA). Beeswax, carnauba wax, isopropyl myristate, sorbitan monoleate (Span 80) and trioleate sorbitan (Span 85) were of cosmetic grade and purchased from Sigma-Aldrich (Missouri, USA). Oleic acid of cosmetic grade was acquired from Labsynth Products Laboratories (Diadema, Brazil), Polysorbate 20

(Tween 20) of cosmetic grade was acquired from Vetec Quimica Fina (Brazil), Polysorbate 80 (Tween 80) of cosmetic grade was acquired from Vetec Quimica Fina (Brazil), and glyceryl monostearate and sesame oil, both of cosmetic grade, were acquired from Croda (Campinas, Brazil). Capric and caprylic acid triglycerides (Captex, cosmetic grade) were purchased from ABITEC Corporation (Ohio, USA). Mineral oil of cosmetic grade was purchased from Penreco (Indiana, USA), and Poloxamer 188 of cosmetic grade was purchased from BASF (Germany).

AVB QUANTIFICATION METHOD

The chromatographic method was adapted from Abid et al.,[24] considering the recommended criteria from the International Council for Harmonization of Technical Requirements for Pharmaceuticals for Human Use (ICH) for validation of chromatographic methods regarding linearity, precision, accuracy, and limits of detection and quantification (ICH Q6B). Specifications: test procedures and acceptance criteria for biotechnological/biological products—scientific guideline. The chromatographic parameters used were: Zorbax Eclipse (Agilent) XDB – C18 column 150mm × 4.6mm, 3.5 μm, with precolumn C18 12.5 × 4.6 mm, 3.5 μm (Agilent), maintained at 30°C. Detection was carried out using a photodiode array at 360 nm. The mobile phase was composed of acetonitrile (ACN) and water (90:10 v/v), at a 1 mL/min^{-1} flow. The injection volume was 10 μL.

SELECTION OF EXCIPIENTS FOR NLC DEVELOPMENT

AVB SOLUBILITY

The solubility of AVB was evaluated in liquid lipids: oleic acid, sesame oil, mineral oil, isopropyl myristate, capric acid triglycerides, and caprylic acid triglycerides. Excess amount of AVB was weighed (150 mg) and transferred to amber glass bottles, where 1 mL of each oil was added. Each oil was tested in triplicates. The samples were each vortexed for 1 minute and then placed in an orbital shaker (KS 4000, IKA®, Germany) at a speed of 150 rpm, at 37°C, for 24 hours. The samples were then filtered through 0.45 μm polyvinylidene fluoride (PVDF) microfiltration membranes, were diluted with 10 mL ACN, and AVB solubility was then quantified by high-performance liquid chromatography (HPLC).

THERMOGRAVIMETRY AND DIFFERENTIAL THERMAL ANALYSIS

The thermal evaluation of AVB and raw lipid excipients, as well as the AVB:excipients physical mixture (1:1 m/m), was carried out in a DTG-60 thermobalance (Shimadzu, Kyoto, Japan), with simultaneous measurement of mass loss (TG/DTG) and melting events (DTA), under a nitrogen atmosphere (50 mL/min^{-1}), with a heating rate of 10 $°C.min^{-1}$, and a temperature range of 25–500°C. Platinum crucibles were used for the analysis of 5 mg of each sample.

FOURIER TRANSFORM INFRARED SPECTROSCOPY

Attenuated total reflectance Fourier transform infrared spectra were obtained on a Varian 640-IR (Varian Medical Systems Inc., Jundiaí, Brazil). AVB, lipid excipients, and

AVB:lipid-based excipients binary mixtures (1:1 m/m) were analyzed at wavelengths of 4,000–600 cm^{-1} with a resolution of 4 cm^{-1}, using attenuated total reflection (ATR). Around 2 ± 1 mg were used to evaluate the solid excipients and 20 uL (about a drop) of the liquids. Each sample was subjected to 64 scans to obtain the spectra.

DEVELOPMENT AND *IN VITRO* CHARACTERIZATION OF THE NANOSTRUCTURED LIPID CARRIERS

NANOSTRUCTURED LIPID CARRIER OBTAINING

After the evaluation of AVB compatibility with NLC excipients, the formulations were obtained by the phase inversion method previously described by Shinoda et al.[25] Water and oil phase components were weighed separately. The lipid, surfactant, and AVB were weighed and then added to the same container. For the water phase, water was weighed in a separate container. Both phases were heated to a temperature of 80–90°C and, subsequently, the water phase was poured into the oil phase under mechanical stirring at 400 rpm and then left to stabilize for 10 minutes. The formulation (Table 1) was submitted to high-pressure homogenization at 400 bar in a LV1 Microfluidizer (Microfluidics Corporation, Massachusetts, USA). 0.5% AVB was added to the oil phase.

PHYSICOCHEMICAL CHARACTERIZATION OF NLCS

The formulations were evaluated regarding their macroscopic aspect, average particle diameter, polydispersity index (PdI), zeta potential, and encapsulation efficiency (EE%). Color, homogeneity, presence, or absence of coalescence or precipitate were visually evaluated. The average diameter and PdI were evaluated by dynamic light scattering using a ZetaSizer Nano S (Malvern Instruments Ltd., Worcestershire, UK) using a 1/40 dilution in ultrapure water. Zeta potential was evaluated by electrophoretic mobility in a ZetaPlus equipment (Brookhaven, New York, USA) using a 1/40 dilution in ultrapure water. The EE% was evaluated by the indirect method, in which 1 mL of the NLC dispersion was centrifuged (SIGMA 3-18K Centrifuge®, SciQuip, Shrewsbury, UK) at 12,000 rpm for 20 minutes. The collected supernatant was diluted with ACN, homogenized, and quantified by HPLC. Drug EE was calculated according to Eq. 1.

$$EE\,(\%) = \frac{\text{Amount of AVB in the NLC}}{\text{Amount of AVB add in the formulation.}} \times 100 \qquad \text{(Eq. 1)}$$

Table I
Percentual Composition of NLC Formulations Evaluated for the Encapsulation of AVB

Composition	F1	F2	F3
Carnauba wax	3.5	3.5	2.5
Isopropyl myristate	1.5	1.5	2.5
Sorbitane trioleate (Span 85)	1.25	1.75	1.89
Polysorbate 80 (Tween 80)	3.75	5.25	5.11
Water	qs 100	qs 100	qs 100

PHYSICAL STABILITY

The physical stability of the selected formulation was evaluated in a Turbiscan Lab Expert analyzer (Formulation Inc., Toulouse, France). The detection head was composed of a pulsed near-infrared light source (k = 850 nm) and transmission and backscattering detectors. The NLC sample was placed in a cylindrical glass tube and scanned throughout the tube height every 30 minutes continuously for 24 hours at 37°C. The stability of the formulation was determined through the variation of backscattering of the sample over the monitored time, using Easysoft© software (Easysoft, Wetherby, United Kingdom).

PHOTOSTABILITY STUDY

Samples of NLC encapsulating AVB, NLC without AVB and of AVB dissolved in ACN (n = 3) were subjected to UVA radiation (3,025 mW/cm²) for 24 hours in a photostability chamber (424 CF, Nova Ética, Brazil) equipped with a near-UV fluorescent lamp (15 W) with a spectral distribution from 320–400 nm and several cool white fluorescent lamps (15 W). The samples collected before irradiation, after 2, 4, 8, and 24 hours of irradiation, and quantifications of AVB were performed by HPLC.

SKIN RETENTION AND PERMEATION

For the *in vitro* study of cutaneous retention in pig ear skin, manual vertical Franz-type static flow cells equipment (Hanson Research, USA) were used under agitation of 300 rpm, at 37°C and a diffusion area of 1.86 cm². The receiving compartment contained 6.7 mL of phosphate-buffered saline (PBS) buffer solution (pH: 7.4) with 5% Tween20, with 1 mL samples being collected at each time point. The 400 μm skin was positioned between the two compartments with the stratum corneum facing up. 18.5 μL of the formulation were applied on the stratum corneum surface to maintain sink conditions (data not shown). Samples were collected at 2, 4, 6, 8, and 24 hours of permeation and were quantified by HPLC. The study was conducted under the norms of research involving animals with protocol CEUA/UFG nr. 105/22.

To evaluate the cutaneous retention of nano encapsulated AVB on the skin surface, the skins were removed from the compartments after 24 hours of exposure and were washed with 2 mL of PBS buffer solution (pH: 7.4) containing 5% Tween 20. Next, tape stripping was performed using adhesive tape to remove the stratum corneum. This procedure was repeated 15 times on each skin, and then the strips were added in 15 mL tube with 5 mL of ACN, homogenized for 2 minutes in a vortex, transferred to the ultrasound bath for 20 minutes, and then filtered through a PVDF membrane (0.45 μm) for quantification by HPLC. Finally, the remaining skin was fragmented, diluted in 5 mL of can, and homogenized for 2 minutes in a vortex. The homogenate was kept under ultrasound for 20 minutes and then filtered (PVDF 0.45 μm). The assay was performed six times, and all samples were quantified by HPLC.

STATISTICAL ANALYSIS

A student's t-test was used to compare the sets of data in Graphpad Prism software version 5.0 (Graphpad Prism Inc., Massachusetts USA), and p values < 0.05 were considered significant.

RESULTS AND DISCUSSION

AVB QUANTIFICATION

The analytical method was able to elute AVB in 3.5 minutes. The presence of two peaks was identified (Figure 1), one at 2.2 minutes corresponding to AVB in its keto form, and the other at 3.4 minutes corresponding to its enol form, as described by Abid et al.[24] The method was linear, with a correlation coefficient $r = 0.9995$, and all points on the curve presented RPD $< 5\%$. Accuracy was in the range of 5% of variation (95–105%). Detection and quantification limits were 0.0509 and 0.1542 μg/mL, respectively. As for selectivity, no changes were observed in the peaks obtained from AVB, in relation to the peaks of the isolated candidate components of the formulations.

AVB SOLUBILITY

AVB showed different solubilities in the liquid lipids: 49.20 ± 2.83 mg/mL^{-1} in oleic acid, 126.79 ± 7.87 mg/mL^{-1} in isopropyl myristate, and 124.85 ± 1.95 mg/mL^{-1} in capric and caprylic acid triglycerides. AVB solubility in mineral oil and sesame oil was 17.22 ± 6.50 mg/mL^{-1} and 45.45 ± 1.57 mg/mL^{-1}, respectively.

THERMAL ANALYSIS (DTA AND TG/DTG)

Figure 2 shows the DTA curves of AVB and the mixture of AVB with lipid-based excipients. The DTA curve of AVB shows a narrow endothermic peak with T_{peak} at 86.45°C. The greatest variations in AVB T_{peak} (29.67–20.69°C) were observed in the binary mixtures with Poloxamer 188, glyceryl monostearate, and beeswax. Anticipations of the AVB

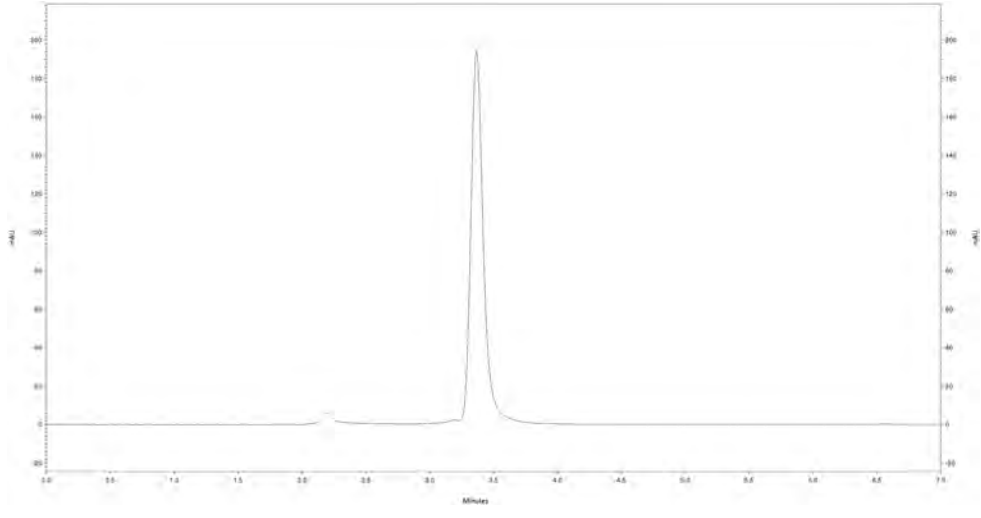

Figure 1. Chromatogram of AVB sample obtained by HPLC. Zorbax Eclipse (Agilent) XDB – C18 column 150mm × 4.6 mm, 3.5 μm, with precolumn C18 12.5 × 4.6 mm, 3.5 μm (Agilent), maintained at 30°C. The mobile phase was composed of ACN and water 90:10, v/v, at a 1 mL/min-1 flow. The injection volume was 10 μL. Sample concentration was 30 μg/mL.1

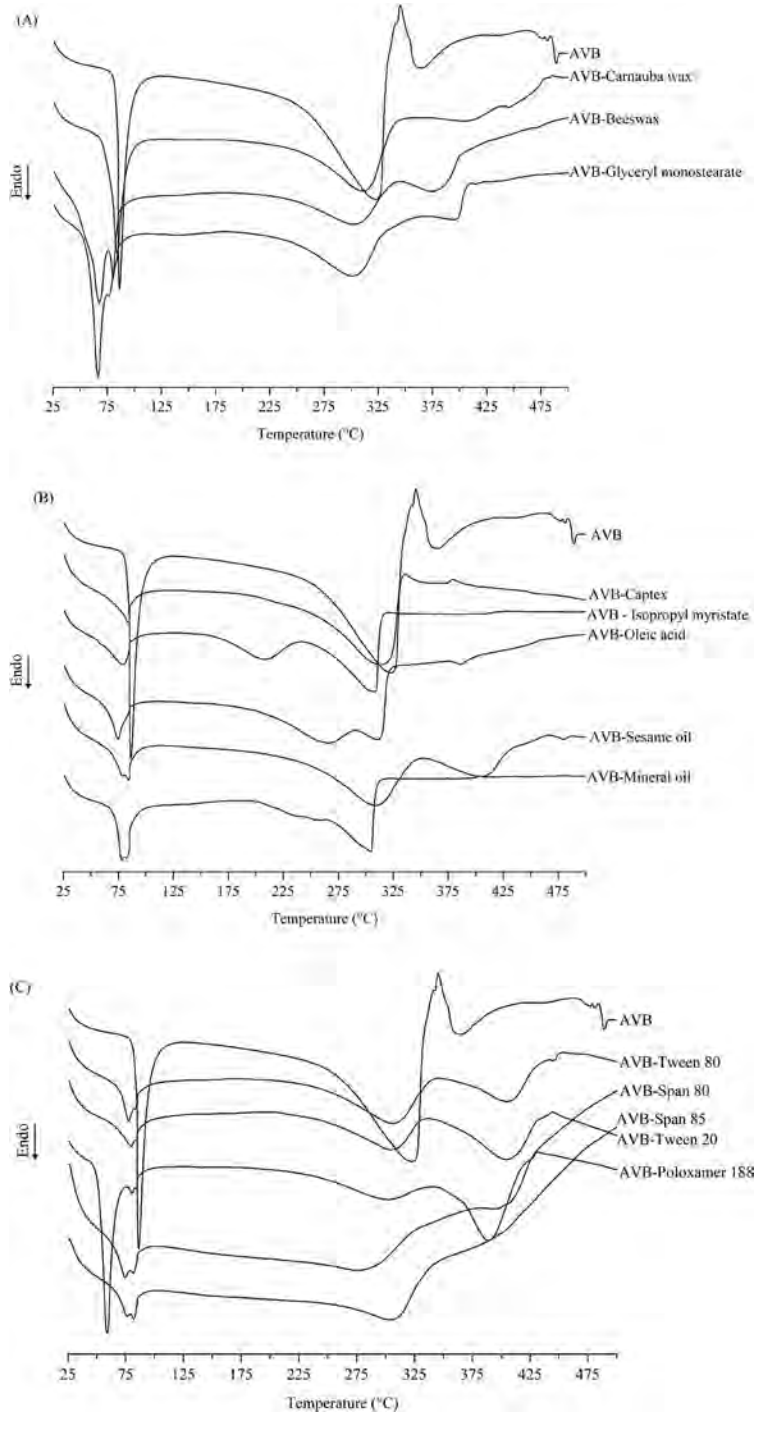

Figure 2. DTA curves of AVB and its binary mixtures 1:1 (m/m) with lipid-based excipients: (A) solid lipids, (B) liquid lipids, and (C) surfactants. Samples were analyzed under nitrogen atmosphere (50 mL/min^{-1}), heating rate of 10°C/min^{-1}, and temperature range of 25–500°C.

melting temperature, between 14.93°C–7.9°C, were observed in the binary mixtures with Tween 80, oleic acid, mineral oil, isopropyl myristate, Tween 20, and Span 80. The smallest variations in the AVB melting temperature (3.74°C–1.63°C) were observed in the binary mixtures with carnauba wax, caprylic and capric acid triglyceride, sesame oil, and Span 85. These changes observed in the endothermic event, in the presence of excipients, may be related to the dissolution of AVB in molten lipids/oils or its solubilization by surfactants.

The mass loss curves of AVB and its binary mixtures with lipid-based excipients are shown in Figure 3. The DTG T_{peak} of the AVB was 323.84°C. The smallest anticipations of the weight loss temperature of AVB (3.26°C at 12.26°C) were observed in the binary mixture with caprylic and capric acid triglyceride, carnauba wax, beeswax, oleic acid, and sesame oil. A greater loss of thermal stability of AVB was observed in the binary mixtures with Poloxamer 188 (anticipation of 24.27°C) and Span 80 (anticipation of 34.25°C). DTG curves of the mixtures with glyceryl monostearate, isopropyl myristate, mineral oil, Tween 80, Tween 20, and Span 85 showed AVB-DTG T_{peak} anticipation between 14.6°C–19.37°C.

FOURIER TRANSFORM INFRARED SPECTROSCOPY

Figure 4 shows the FTIR spectra of AVB, the binary mixture of AVB with solid lipids (Figure 4A), liquid lipids (Figure 4B), and surfactants (Figure 4C). The FTIR spectrum of the isolated AVB showed groups at 2,963 cm^{-1} (C-H bond of aliphatic groups), 1,666 cm^{-1} (aryl ketone), 1560–1500 cm^{-1} (C-C-C = O and OH bending), and 1,256 cm^{-1} (aryl alkyl ether). These groups have been correlated to the photoprotective activity of AVB.[26,27]The characteristic FTIR peaks of AVB were present in the binary mixtures with solid lipids (Figure 4A) and liquid lipids (Figure 4B). In the spectra of mixtures of AVB with all tested surfactants (Figure 4C), the band in 2,963 cm^{-1} was not observed. In the mixtures of AVB with Tween 80 and Tween 20, no changes were observed in 1,666 cm^{-1} and 1,256 cm^{-1}, while in the AVB-Poloxamer 188 mixture, a decrease in the intensity of these bands was observed. Binary mixtures of AVB with Span 80 and Span 85 showed similar FTIR spectra to the ones observed for the isolated excipients, with bands overlapping in 1,666 cm^{-1} and 1,256 cm^{-1}. No changes were observed in the absorption of the enol bands in this region for all excipients.

The interpretations of results given by the analysis methods are extremely complex. Generally, interactions are observed, but by themselves they do not allow us to reach a conclusion of whether components were incompatible. Therefore, it is necessary to carry out analyses using different methods and interpret them together. The interactions observed in DTA may indicate dissolution and/or solubilization of the active ingredient in the lipid and surfactant excipients, not necessarily incompatibilities between them. In the development of delivery systems, these phenomena of physical interaction between active and matrix-forming components are often required to improve parameters such as: solubility, EE, active loading, and stability.[19,20]

In DTG, anticipations of mass loss may also be related to these physical interactions. Also, at these high temperatures (which are much higher than the production and storage temperatures of these formulations), there may be oxidation of the lipid material (or other degradation phenomena), and these degradation products interfere with the mass loss temperature of the product. However, it does not necessarily indicate an interaction of the incompatibility type between the active ingredient and the excipients evaluated. In these

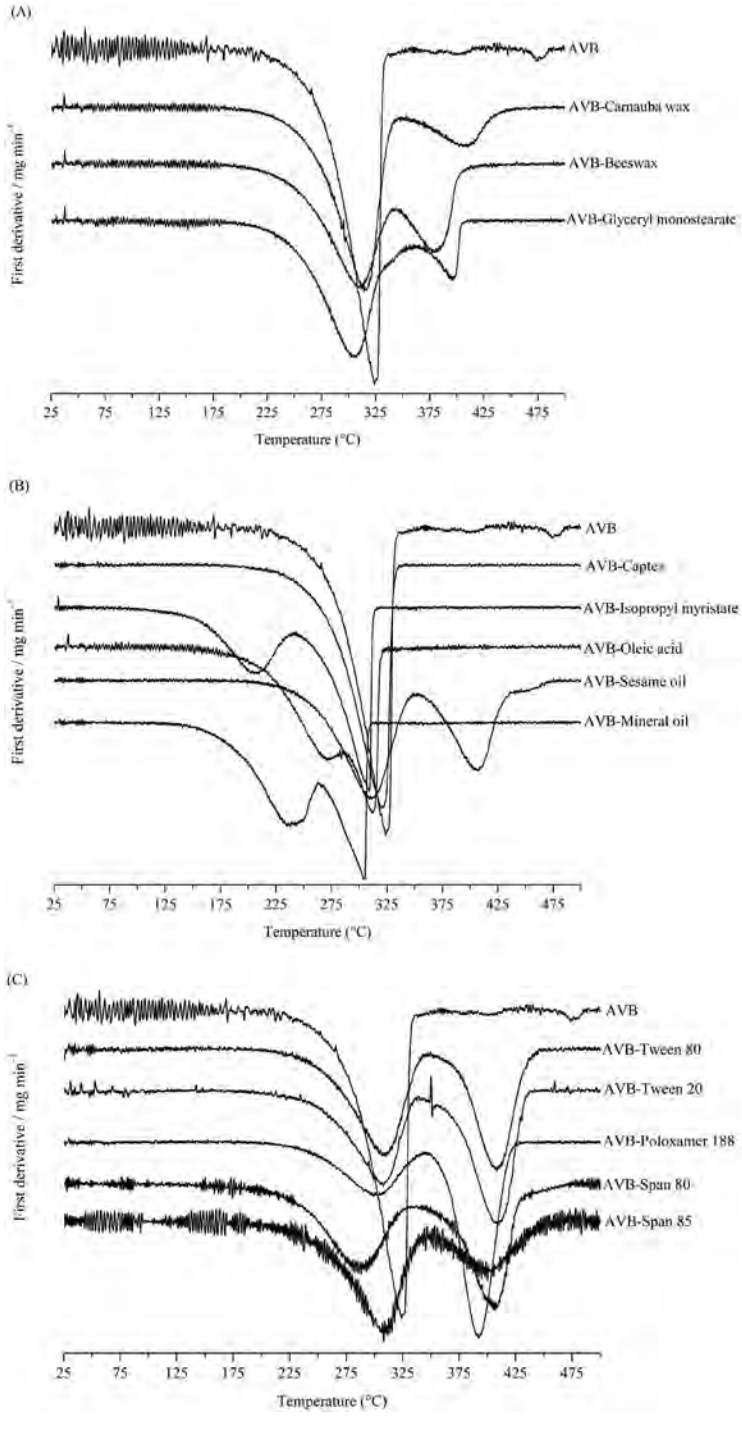

Figure 3. DTG curves of AVB and its binary mixtures 1:1 (m/m) with lipid-based excipients: (A) solid lipids, (B) liquid lipids, and (C) surfactants. Samples were analyzed under a nitrogen atmosphere (50 mL/min^{-1}), heating rate of 1°C/min^{-1}, and temperature range of 25–500 °C.

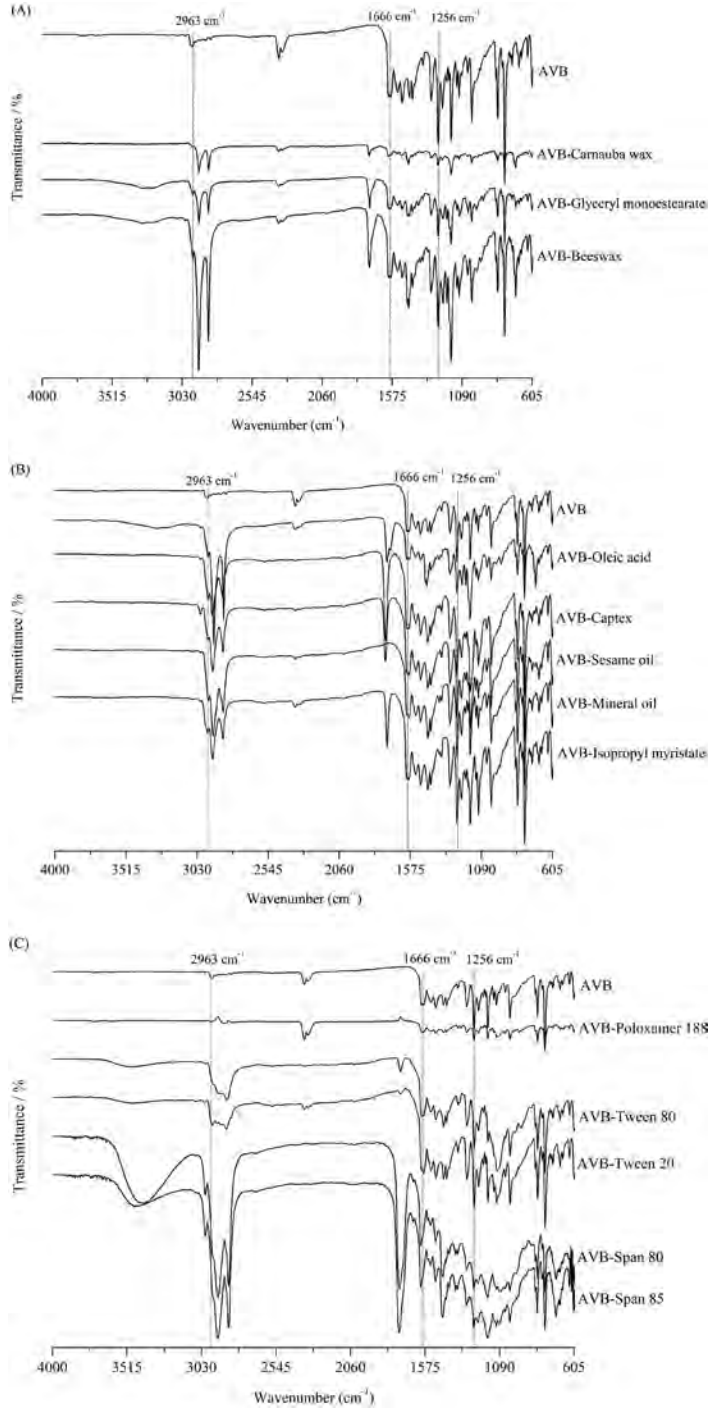

Figure 4. FTIR spectrum of avobenzone (AVB) and its binary mixtures 1:1 (m/m) with lipid-based excipients: (A) solid lipids, (B) liquid lipids and (C) surfactants. Spectra were recorded in a Varian 640-IR FTIR (Varian Inc., Brazil) at wavelengths 4000-600 cm^{-1} with a resolution of 4 cm^{-1}, using an ATR.

cases, the use of methods that evaluate molecular interactions at a chemical level can help to elucidate or facilitate the identification of the nature of these interactions. No major changes were observed in the FTIR data, which would indicate incompatibility between the active ingredient and the excipients evaluated. Therefore, it can be suggested that the changes (interactions) observed with the DTA/TG-DTG and FTIR analyzes are indicative of changes in the physical state of the active ingredient, which is dissolved or solubilized in the melted/heated excipients.

PREPARATION OF THE NANOSTRUCTURED LIPID CARRIERS

The compatibility experiments, using commonly available excipients for the preparation of NLCs, demonstrated that carnauba wax, isopropyl myristate, Span 85, and Tween 80 were suitable for the preparation of NLCs encapsulating AVB. Three formulations with different proportions of the selected lipid-based excipients (solid-lipid, liquid-lipid, and surfactant and cosurfactant) were tested for the preparation of the NLCs (Table I).

Initially, 5% of surfactants were evaluated in relation to the total formulation (F1). For F2 and F3 formulations, 7% of surfactants were tested for the preparation for NLCs. The ratio of the surfactants used to obtain the NLCs was based on the required hydrophilic–lipophilic balance for the formulation (mathematical model/data not shown). Formulations F1, F2, and F3 showed the formation of emulsions. After 24 hours, the presence of agglomerates, indicating instability, were observed in F2. F3 formulation remained without signs of instability, showing a milky and homogeneous appearance, with average particle size and PdI of 138.9 ± 43.86 and 0.144 ± 0.03, respectively. After 7 days, however, oil droplets were observed, indicating a coalescence process. The mean particle diameter and PdI after 7 days were 145.9 ± 57.32 and 0.196 ± 0.04. F3 was then subjected to 3 cycles of homogenization at 400 bar, and again evaluated for a period of 7 days (Table II). The high-pressure homogenization technique was chosen because of its feasibility of scale-up and for producing particles of smaller sizes compared to other techniques, thus contributing to the improvement of formulation stability.[28] After this new homogenization cycle, formulation F3 did not show changes in the macroscopic aspect. Mean diameter and PdI, shown in Table II, did not show statistical differences during the 7 days of evaluation ($p > 0.05$). The EE% of AVB in the freshly prepared samples was 72.8% ± 1.8%. F3 formulation was then chosen as the most macroscopically stable, and with acceptable diameter and PdI for encapsulation of AVB and was then further investigated.

Table II
Mean Diameter (MD), in nm, and Polydispersity Index (PdI) of the NLC Formulations (F3) Submitted to Continuous Microfluidization Cycles at 400 Bar.

Day	Cycle 1		Cycle 2		Cycle 3	
	MD ± sd	PdI ± sd	MD ± sd	PdI ± sd	MD ± sd	PdI ± sd
0	148 ± 42	0.15 ± 0.02	138 ± 45	0.14 ± 0.03	139 ± 45	0.15 ± 0.03
1	153 ± 43	0.15 ± 0.05	137 ± 47	0.17 ± 0.04	137 ± 46	0.15 ± 0.03
5	160 ± 44	0.17 ± 0.03	182 ± 56	0.18 ± 0.04	141 ± 49	0.14 ± 0.02
7	171 ± 38	0.16 ± 0.06	146 ± 51	0.16 ± 0.05	144 ± 50	0.17 ± 0.03

*Samples were monitored for 7d after preparation. N = 3, $p > 0.05$.

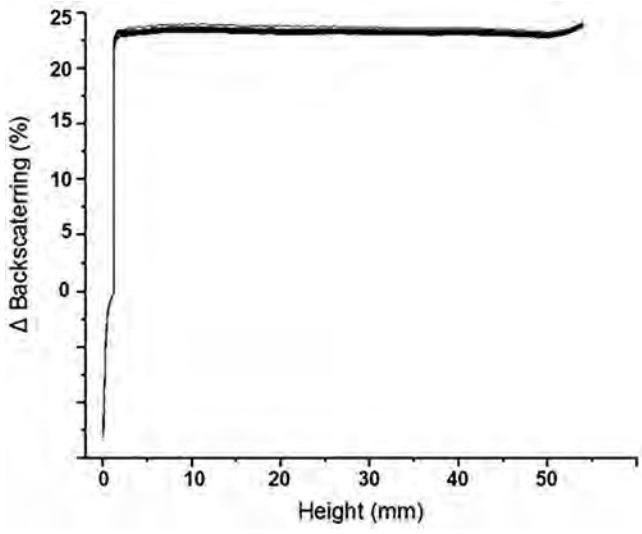

Figure 5. Variation of backscattering profile of the F3 formulation, obtained by scanning the NLC sample every 1h, for 24h, at 37°C, using Turbiscan Lab.

CHARACTERIZATION OF THE NLCS

TURBISCAN

F3 formulation was analyzed by dynamic turbidimetry for assessment of its physical stability. In the graph results (Figure 5), the x-axis represents a residual percentage of backscattering light, and the y-axis represents the height of the tube containing the sample. This graph allows the comparative verification of the variation profiles of the backscattered light at different times and sample heights; if the profiles overlap at different times, the product can be considered stable. The occurrence of destabilization phenomena (aggregation and flocculation) and phase separation modify the interaction of the light beam with the formulation dispersant, causing an increase or decrease in the intensity of transmission and backscattering due to the variation in the size of the particles. For F3, a variation of backscattering of $< \pm 1\%$ was observed, demonstrating the physical stability of the formulation.[29]

FORMULATION PHYSICOCHEMICAL STABILITY

The results of MD and PdI of the formulation were monitored for 30 days to corroborate the results of physical stability obtained through the backscattering analysis. No aggregation, flocculation, or phase separation were observed. As shown in Figure 6, no significant changes in the average particle size and PdI were measured ($p > 0.05$). A statistically significant difference was, however, observed in the NLCs zeta potential on day 30 ($p < 0, 05$). This change is believed not to influence the steric stability of the particles in the formulation, since zeta values larger than 20 mV tend to be sufficient to maintain long-term stability (as demonstrated by Medeiros et al.[30]) after the preparation of NLCs encapsulating an UV filter, prepared using carnauba wax, and capric/caprylic acid triglycerides.

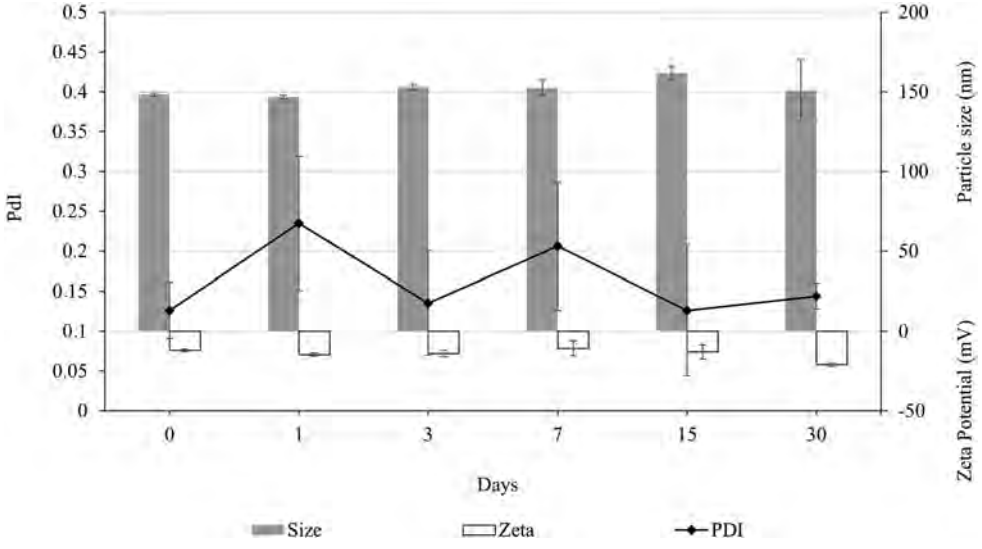

Figure 6. Average diameter, PdI and zeta potential of AVB-NLC (F3) evaluated during 30d at room temperature. Values represent mean ± S.D (n = 3).

PHOTOSTABILITY STUDY

The selection of ACN as the solvent for the positive control was based both on its use as a diluent and mobile phase component of the HPLC method, as well as on other AVB photostability studies described in the literature.[31] It was demonstrated that AVB is predominantly found in the enol form, and after exposure to radiation it presents photo-instability converting into the keto form. In addition to exposure time and concentration, photo-instability was also dependent on the type of solvent. In methanol, chloroform, and acetone, there was no significant photoisomerization of AVB under the conditions tested.[32,33] In agreement with these findings, our photostability study showed significant differences between exposed and unexposed samples and between samples of NLC containing AVB when compared to samples of AVB in ACN (positive control). Formulations containing free AVB after UVA irradiation demonstrated a 50–70% decrease in the filter content, while encapsulated AVB showed a maximum 5% decrease. Figure 7 shows the evaluation AVB-NLC and AVB in ACN exposed to UVA radiation for a period of 24 hours. Under the experimental conditions, the samples showed significant differences ($p < 0.05$) when compared.

In Figure 7, it is possible to observe that the AVB in ACN showed a decrease in its content, reaching 50% in 24 hours. On the other hand, in both the NLCs containing AVB exposed or not to UV radiation, the AVB content was maintained during the period of 24 hours, which suggests that the AVB presented a photostable behavior when encapsulated in NLC. As observed in previous works,[32] the presence of cinnamic-acid derivate filters can increase the formulation photostability. Since some filters affect the stability of others, the resulting stability may chance in different filter combinations, and this could be the case of carnauba wax, which presents in its composition p-methoxycinnamic diesters.[32,34] Other works have shown that when avobenzone sunscreens were nanoencapsulated in nanocapsules or nanoemulsion, photodegradation was lower than when compared to traditional emulsions.[35]

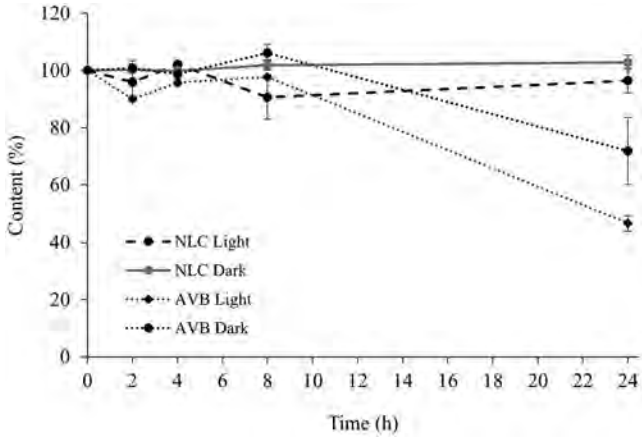

Figure 7. Photostability of free and NLC-encapsulated AVO (F3). Samples were exposed for 24h and subjected to UVA radiation (3,025 mW/cm²) for 24h in a photostability chamber.

In addition to photostability, the increase in the photoprotective properties of creams based on lipid nanoparticles versus conventional creams has already been described.[36,37] Liposomes and lipid nanoparticles have increased AVB photoprotection by 40%.[38] The increased UV protection is attributed to the synergistic effect of the lipid matrix. Isopropyl myristate has been shown to be the most appropriate lipid-excipient for ensuring AVB photostability.[30] Similarly, the entrapment of avobenzone in lipid microparticles have been demonstrated as an effective strategy to reduce the photo-instability of AVO after irradiation.[39] Normally nanoparticles act as UV physical filters, due to their efficient light scattering properties, which promotes a synergistic UV protection effect with the encapsulated UV chemical filter. Additionally, depending on their composition, lipid components may present antioxidant activity and add to the photostabilisation effect of the encapsulated material.[39] Understanding photodegradation pathways when using photosensitive filters is a crucial step in the design of photoprotective formulations. The combination of several strategies, including encapsulation, antioxidants, photostabilizing substances, and suppressors can be used as effective tools for photoprotection.[39-41]

SKIN RETENTION AND PERMEATION

Recently, the Food and Drug Administration has evidenced that various UV filters can diffuse into systemic circulation and cause harm.[42] The lipophilic character and permeability properties of AVB, such as its lipophilicity, could favor its diffusion through biological membranes. AVB pKa is between 9.60–9.80. At both physiological pH values and cutaneous pH, there will be a clear dominance of AVB in the nonionized state, which is predictive of high permeation across biological barriers.[43,44]

The effectiveness of a sunscreen depends on its ability to keep UV filter molecules in the outermost region of the skin. The ideal sunscreen should have low permeation properties and high accumulation capacity in this region.[39] Here, we demonstrated that encapsulation in NLCs promoted greater skin retention of AVB, showing a significantly ($p < 0.05$) higher retention on the skin surface when compared to the concentration that penetrated the stratum corneum (Figure 8).

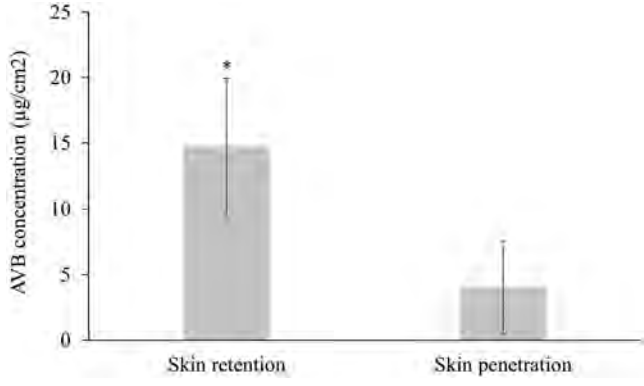

Figure 8. Amount of AVB-NLC (F3) retained in the cutaneous surface and permeated through the skin after 24h of the experiment. The pig ear skin model was used in Franz-type static flow cells. Medium was maintained at 300 rpm, 37°C. The diffusion area was 1.86 cm^2. The receiving compartment contained PBS buffer solution (pH: 7.4) with 5% Tween 20, with 1 mL samples being collected at each time point.

The structure of the nanocarriers has also been shown to influence penetration through the skin. Semisolid formulations containing nanocapsules provided greater retention in the stratum corneum compared to semisolids containing benzophenone-3 in.the free form.[21] Gels containing oxybenzone nanoencapsulated in solid-lipid nanoparticles, and confocal microscopy was used to assess the localization of the formulations on the skin. The authors demonstrated that there was a reduction in the penetration of sunscreen when nanoencapsulated.[22] Cutaneous retentions of AVB entrapped in cyclodextrin was investigated. In their work, the authors demonstrated that the stratum corneum contained most of the absorbed UV filter.[45,46] The proportion of the applied dose that was diffused into the stratum corneum for the sunscreen cream with nonencapsulated sunscreen agents was about 30.3% for AVB. The cream with microencapsulated UV filters reduced *in vivo* skin penetration by a statistically significant amount. In the deeper stratum corneum layers, the lipid microparticles inhibitory effect on permeability was more pronounced (45–56.3% decrease).[39]

Together, the results show the advantages of encapsulating AVB in NLCs. In the pathway to incorporating AVB-NLCs in a cosmetic base to develop a commercially available product, the AVB release, stability of the nanocarriers once incorporated in a cosmetic base stability, long-term stability of the formulation, and scaling-up should be investigated.

CONCLUSION

Based on the results of the active and excipient interaction studies using DTA and TG/DTG and FTIR, it was possible to rationally select the components for the preparation of NLCs. Carnauba wax, isopropyl myristate, Span 85, and Tween 80 were tested for the preparation of NLCs and encapsulation of AVB. NLCs prepared with carnauba wax showed less loss of active content in the face of exposure to UVA radiation (maximum 5%, compared to 50% of loss of AVB in ACN) and greater retention on the skin surface, when compared to the AVB that penetrated the stratum corneum. These results demonstrate that the incorporation of this type of active in lipid nanoparticles can contribute both to improve the efficiency of sunscreen activity and to reduce the permeation of these molecules in the skin.

STATEMENT OF CONTRIBUTION

L.A.D.S D.G.A.D. conceived the study and oversaw the overall direction and planning. I.P.S. carried out the experiments with the help of A.C.T.L., B.C.C.R., E.R.C., and L.M.S. for the development and characterization of lipid carriers, the photostability study, thermal analysis, and *in vitro* skin permeation, respectively. T.L.N. aided in interpreting the results and worked on the manuscript. E.M.L. provided material and equipment support for the research.

ACKNOWLEDGEMENTS

This work was financed by Cordenação de Aperfeiçoamento de Pessoal de Nível Superior (CAPES) and Conselho Nacional de Desenvolvimento Científico e Tecnológico.

REFERENCES

(1) Ciążyńska M, Kamińska-Winciorek G, Lange D, et al. The incidence and clinical analysis of non-melanoma skin cancer. *Sci Rep.* 2021;**11**(1):4337. doi:10.1038/s41598-021-83502-8

(2) Lomas A, Leonardi-Bee J, Bath-Hextall F. A systematic review of worldwide incidence of nonmelanoma skin cancer. *Br J Dermatol.* British Association of Dermatologists. 2012;**166**(5):1069–1080. doi:10.1111/j.1365-2133.2012.10830.x

(3) Hu W, Fang L, Ni R, Zhang H, Pan G. Changing trends in the disease burden of non-melanoma skin cancer globally from 1990 to 2019 and its predicted level in 25 years. *BMC Cancer.* 2022;**22**(1):836. doi:10.1186/s12885-022-09940-3

(4) Sander M, Sander M, Burbidge T, Beecker J. The efficacy and safety of sunscreen use for the prevention of skin cancer. *CMAJ.* 2020;**192**(50):E1802–E1808. doi:10.1503/cmaj.201085

(5) Fourtanier A, Moyal D, Seite S. UVA filters in sun-protection products: regulatory and biological aspects. *Photochem Photobiol Sci.* 2012;**11**(1):81–89. doi:10.1039/c1pp05152k

(6) Marrot L, Meunier JR. Skin DNA photodamage and its biological consequences. *J Am Acad Dermatol.* 2008;**58**(5)(suppl 2):S139–S148. doi:10.1016/j.jaad.2007.12.007

(7) Mahmoud BH, Ruvolo E, Hexsel CL, et al. Impact of long-wavelength UVA and visible light on melanocompetent skin. *J Invest Dermatol.* 2010;**130**(8):2092–2097. doi:10.1038/jid.2010.95

(8) Lan C-CE, Hung YT, Fang AH, Ching-Shuang W. Effects of irradiance on UVA-induced skin aging. *J Dermatol Sci.* 2019;**94**(1):220–228. doi:10.1016/j.jdermsci.2019.03.005

(9) González S, Fernández-Lorente M, Gilaberte-Calzada Y. The latest on skin photoprotection. *Clin Dermatol.* 2008;**26**(6):614–626. doi:10.1016/j.clindermatol.2007.09.010

(10) Food and Drug Administration (FDA), Department of Health and Human Services. Guidance for industry: maximal usage trails for topical active ingredients being considered for inclusion in an over-the-counter monograph: study elements and considerations. *FDA Website.* 2018. Accessed 8/23/2023. https://www.fda.gov/regulatory-information/search-fda-guidance-documents/maximal-usage-trials-topically-applied-active-ingredients-being-considered-inclusion-over-counter.

(11) Mturi GJ, Martincigh BS. Photostability of the sunscreening agent 4-tert-butyl-4′-methoxydibenzoylmethane (avobenzone) in solvents of different polarity and proticity. *J Photochem Photobiol A.* 2008;**200**(2-3):410–420. doi:10.1016/j.jphotochem.2008.09.007

(12) Durango S, Castañeda S, Vallejo J, Gallardo C. Solvent effect on photostability of butyl methoxy di benzoyl methane formulated in solution and emulsion. *Int J Pharm Pharm Sci.* 2015;7:181–186.

(13) Weiss-Angeli V, Poletto FS, Zancan LR, Baldasso F, Pohlmann AR, Guterres SS. Nanocapsules of Octyl Methoxycinnamate containing quercetin delayed the photodegradation of both components under ultraviolet A radiation. *J Biomed Nanotechnol.* 2008;4:80–89.

(14) Niculae G, Badea N, Meghea A, Oprea O, Lacatusu I. Coencapsulation of butyl-methoxydibenzoylmethane and Octocrylene into lipid nanocarriers: UV performance, photostability and in vitro release. *Photochem Photobiol.* 2013;**89**(5):1085–1094. doi:10.1111/php.12117

(15) Beraldo-de-Araújo VL, Beraldo-de-Araújo A, Costa JSR, et al. Excipient-excipient interactions in the development of nanocarriers: an innovative statistical approach for formulation decisions. *Sci Rep.* 2019;**9**(1):10738. doi:10.1038/s41598-019-47270-w

(16) Wu H, Cui Z, Huo Y, et al. Influence of drug-carrier compatibility and preparation method on the properties of paclitaxel-loaded lipid liquid crystalline nanoparticles. *J Pharm Sci.* 2021;**110**(7):2800–2807. doi:10.1016/j.xphs.2021.03.016

(17) Mitchell MJ, Billingsley MM, Haley RM, Wechsler ME, Peppas NA. Engineering precision nanoparticles for drug delivery. *Nat Rev Drug Discov.* 2021;**20**(2):101–124. doi:10.1038/s41573-020-0090-8

(18) Johnson LT, Zhang D, Zhou K, et al. Lipid nanoparticle (LNP) chemistry can endow unique in vivo RNA delivery fates within the liver that alter therapeutic outcomes in a cancer model. *Mol Pharm.* 2022;**19**(11):3973–3986. doi:10.1021/acs.molpharmaceut.2c00442

(19) Silva LAD, Cintra ER, Alonso ECP, et al. Selection of excipients for the development of carvedilol loaded lipid-based drug delivery systems. *J Therm Anal Calorim.* 2017;**130**(3):1593–1604. doi:10.1007/s10973-017-6380-7

(20) Siew A. The importance of lipid screening in the development of lipid-based formulations. *Pharm Technol.* 2016;**40**:20.

(21) Paese K, Jäger A, Poletto FS, et al. Semisolid formulation containing a nanoencapsulated sunscreen: effectiveness, in vitro photostability and immune response. *J Biomed Nanotechnol.* 2009;**5**(3):240–246. doi:10.1166/jbn.2009.1028

(22) Gulbake A, Jain A, Khare P, Jain SK. Solid lipid nanoparticles bearing oxybenzone: in-vitro and in-vivo evaluation. *J Microencapsul.* 2010;**27**(3):226–233. doi:10.1080/02652040903067844

(23) Wang J, Pan L, Wu S, et al. Recent advances on endocrine disrupting effects of UV filters. *Int J Environ Res Public Health.* 2016;**13**(8):782. doi:10.3390/ijerph13080782

(24) Abid AR, Marciniak B, Pędziński T, Shahid M. Photo-stability and photo-sensitizing characterization of selected sunscreens' ingredients. *J Photochem Photobiol A.* 2017;**332**:241–250. doi:10.1016/j.jphotochem.2016.08.036

(25) Shinoda K, Saito H. The Stability of O/W type emulsions as functions of temperature and the HLB of emulsifiers: the emulsification by PIT-method. *J Colloid Interface Sci.* 1969;**30**(2):258–263. doi:10.1016/S0021-9797(69)80012-3

(26) Dornelas C, Rodrigues K, Padilha R, et al. Characterization of intercalation compounds of sunscreens in a bentonite organoclay. *J Chem Pharm Res.* 2015;**7**:816–821.

(27) Yuan L, Li S, Huo D, et al. Studies on the preparation and photostability of avobenzone and (2-hydroxy) propyl-β-cyclodextrin inclusion complex. *J Photochem Photobiol A.* 2019;**369**:174–180. doi:10.1016/j.jphotochem.2018.09.036

(28) Yadav KS, Kale K. High pressure homogenizer in pharmaceuticals: understanding its critical processing parameters and applications. *J Pharm Innov.* 2020;**15**(4):690–701. doi:10.1007/s12247-019-09413-4

(29) Celia C, Locatelli M, Cilurzo F, et al. Long term stability evaluation of prostacyclin released from biomedical device through Turbiscan lab expert. *Med Chem.* 2015;**11**(4):391–399. doi:10.2174/1573406410666141110153502

(30) Medeiros TS, Moreira LMCC, Oliveira TMT, et al. Bemotrizinol-loaded carnauba wax-based nanostructured lipid carriers for sunscreen: optimization, characterization, and in vitro evaluation. *AAPS PharmSciTech.* 2020;**21**(8):288. doi:10.1208/s12249-020-01821-x

(31) Vallejo JJ, Mesa M, Gallardo C. Evaluation of the avobenzone photostability in solvents used in cosmetic formulations. *Vitae.* 2011;**18**(1):63–71. doi:10.17533/udea.vitae.8778

(32) Chatelain E, Gabard B. Photostabilization of butyl methoxydibenzoylmethane (avobenzone) and ethylhexyl methoxycinnamate by Bis-ethylhexyloxyphenol methoxyphenyl triazine (Tinosorb S), a New UV

Broadband Filter. *Photochem Photobiol.* 2001;**74**(3):401–406. doi:10.1562/0031-8655(2001)074<0401:pobmaa>2.0.co;2

(33) Hanno I, Anselmi C, Bouchemal K. Polyamide nanocapsules and nano-emulsions containing Parsol® MCX and Parsol® 1789: in vitro release, ex vivo skin penetration and photo-stability studies. *Pharm Res.* 2012;**29**(2):559–573. doi:10.1007/s11095-011-0592-5

(34) Freitas CAS, Vieira ÍG, Sousa PHG, Muniz CR, Gonzaga MLC, Guedes MIF. Carnauba wax p-methoxycinnamic diesters: characterisation, antioxidant activity and simulated gastrointestinal digestion followed by in vitro bioaccessibility. *Food Chem.* 2016;**196**:1293–1300. doi:10.1016/j.foodchem.2015.10.101

(35) Lacatusu I, Badea N, Murariu A, Bojin D, Meghea A. Effect of UV sunscreens loaded in solid lipid nanoparticles: A combinated SPF assay and photostability. *Mol Cryst Liq Cryst.* 2010;**523**(1):247/[819]–259/[831]. doi:10.1080/15421401003719928

(36) Lacatusu I, Badea N, Murariu A, Meghea A. The encapsulation effect of UV molecular absorbers into biocompatible lipid nanoparticles. *Nanoscale Res Lett.* 2011;**6**(1):73. doi:10.1186/1556-276X-6-73

(37) Caldas AR, Faria MJ, Ribeiro A, et al. Avobenzone-loaded and omega-3-enriched lipid formulations for production of UV blocking sunscreen gels and textiles. *J Mol Liq.* 2021;**342**:116965. doi:10.1016/j.molliq.2021.116965

(38) Scalia S, Coppi G, Iannuccelli V. Microencapsulation of a cyclodextrin complex of the UV filter, butyl methoxydibenzoylmethane: in vivo skin penetration studies. *J Pharm Biomed Anal.* 2011;**54**(2):345–350. doi:10.1016/j.jpba.2010.09.018

(39) Gholap AD, Sayyad SF, Hatvate NT, et al. Drug delivery strategies for avobenzone: A case study of photostabilization. *Pharmaceutics.* 2023;**15**(3):1–37. doi:10.3390/pharmaceutics15031008

(40) Food and Drug Administration (FDA). Sunscreen drug products for over-the counter human use, Department of Health and Human Services. *Fed Regist.* 2019;**84**:38.

(41) Yang Y, Ako-Adounvo AM, Wang J, et al. In vitro testing of sunscreens for dermal absorption: A platform for product selection for maximal usage clinical trials. *J Invest Dermatol.* 2020;**140**(12):2487–2495. doi:10.1016/j.jid.2020.04.009

(42) Martins RM, Martins SS, Barbosa GLF, e Silva N, Fonseca MJV, Freitas LAPd. Natural component and solid lipid microparticles of solar filter in sunscreen: photoprotective and photostability effect enhancement. *J Drug Deliv Sci Technol.* 2023;**88**:1–10. doi:10.1016/j.jddst.2023.104860

(43) Hiller J, Klotz K, Meyer S, et al. Systemic availability of lipophilic organic UV filters through dermal sunscreen exposure. *Environ Int.* 2019;132. doi:10.1016/j.envint.2019.105068

(44) Scalia S, Mezzena M. Photostabilization effect of quercetin on the UV filter combination, butyl methoxydibenzoylmethane-Octyl Methoxycinnamate. *Photochem Photobiol.* 2010;**86**(2):273–278. doi:10.1111/j.1751-1097.2009.00655.x

(45) Li CC, Lin LH, Lee HT, Tsai JR. Avobenzone encapsulated in modified dextrin for improved UV protection and reduced skin penetration. *Chemical Papers.* 2016;**70**(6):840–847. doi:10.1515/chempap-2016-0021

(46) Scalia S, Mezzena M, Ramaccini D. Encapsulation of the UV filters ethylhexyl methoxycinnamate and butyl methoxydibenzoylmethane in lipid microparticles: effect on in vivo human skin permeation. *Skin Pharmacol Physiol.* 2011;**24**(4):182–189. doi:10.1159/000324054